

Interaction between Crosswind and Aviation-Fuel Fire Engulfing an Aircraft – A Numerical Study

Hui Ying WANG and Guo Da WANG
Institut P², Fluides, Thermique, Combustion

CNRS-UPR3346, ENSMA, Université de Poitiers, BP 40109 F86961 Futuroscope Chasseneuil
Cedex, France

1 Previous studies

Aviation liquid fuel is volatilised to form a cloud of combustible mixture, with subsequent gas-phase ignition and establishment of a vapour cloud fire. Large fully turbulent fires, which result as a consequence of an aircraft accident, pose a severe hazard to the occupants and cargo. Intensive research has been carried over decades on the pool fires in crossflow [1], though only a small proportion of the work has looked specifically at large-scale pool fires [2]. Presently, analysis of these hazards is primarily limited to characterization of the fire in the absence of other influencing factors such as wind condition and engulfed objects [3, 4].

2 Objective of this work

A video camera from an accident of the aircraft due to engine failure is shown in Figure 1. In large-scale hydrocarbon fires, higher soot levels result in radiation blockage effects around the perimeter of large fire plumes: this yields a drastic reduction in the radiative loss fraction. There are other complications deriving from the intermittency of the behaviour, with luminous regions of efficient combustion appearing randomly in the outer surface of the fire according to the turbulent fluctuations in the fire plume. The burnthrough time of a metallic fuselage depends strongly on external heat flux from a post crash fire, to the fuselage with multilayer including skin, thermo-acoustic insulation, air layer and cabin wall. Moreover, fire resistance of aircraft structure elements depends on the radiation heat transfer from the flames to aircraft skin which is greatly affected by soot production. We have attempted to provide an entirely tractable solution for engineering calculations such as aircraft fires. The availability of such simulation can provide cost-effective alternatives by reducing the number of large-scale tests necessary to develop fire protection requirements or standards.

Schematic diagram of a pool fire engulfing an aircraft and coordinate system in the numerical simulation are shown in Figure 2. The calculations were performed using a computational mesh, which was made up of 200 x 200 x 250 cells with overall dimension of 90 m in length (x), 90 m in width (y) and 100 m in height (z). Influence of the deviation in the wind speed on the behavior of the fire is studied by taking into account a speed range of 0-10 m/s.



Figure 1. Video camera from a real aircraft fire situation

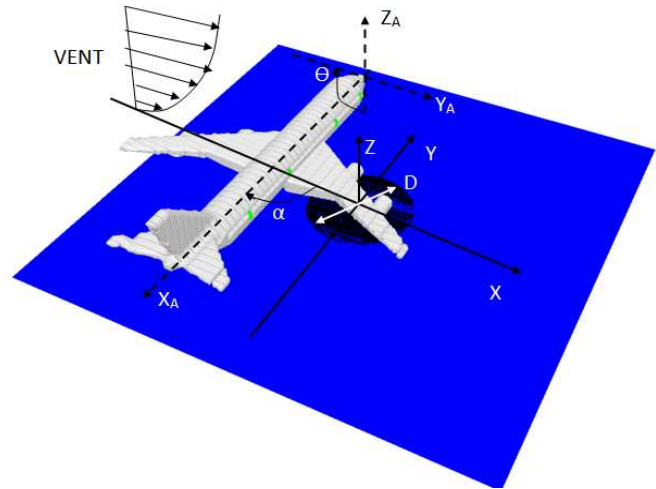


Figure 2. Schematic diagram of the occurrence of large fires engulfing an aircraft and coordinate system

3 Theoretical analysis

Large Eddy Simulation (LES) for the fluid dynamic equations of three-dimensional elliptic flow is coupled with an Eddy Dissipation Concept, allowing to the simulation of turbulent flame. The basis of the analysis is the conservation equations of mass, momentum, energy and species, a set of three-dimensional elliptic, time-dependent Navier-Stokes equations. A dynamic modelling method is applied to obtain appropriate value of the EDC coefficient, allowing to take into account the mass transfer rate between the fine structures and the bulk of the fluid.

Soot is the dominant influence on the absorption coefficient in large fires, and it has been established that the majority of the radiation in fire plume (>90%) is derived from the visible part of the flame, where soot particles are radiating heat. A radiative transfer equation is solved by using a discrete ordinates method [5]. The effect of soot concentration on radiation is included by adding the radiation coefficient of soot into that of gas. The current model uses a classic principle of smoke point to relate soot production to material properties [6]. For the phase coupling conditions, the vaporization rate of condensed fuel is derived from a mass transfer number.

4 Results and discussion

Large-scale (>10 m) liquid hydrocarbon pool fires engulfing aircraft are difficult to analyze experimentally because of the sheer scale of the fire and the instrumentation difficulty. It is relatively easy task of obtaining experimental data for an intermediate pool-like fire, allowing a comparison between prediction and experiment.

A free pool-like fire [3] is stabilized on a horizontal rectangular porous burner with a 0.25 m long (x) by 0.4 m wide (y) slot with a heat release rate of 36 kW. In general, the large scale structure that is controlled by the inviscid terms can be completely described when this characteristic length is spanned by roughly ten computational cells. This implies that adequate resolution of the fire plume in large-scale can be achieved with a spatial resolution of about 0.025 m. Grid refinement (about 1.5 times as fine) studies were performed for checking the influence of number of grid cells on the predicted results. Figures 3, 4 and 5 show that the general shapes of the experimentally-determined temperature, velocity and turbulent fluctuations profiles are correctly reproduced by the numerical model.

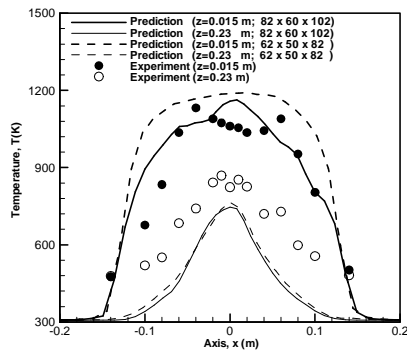


Figure 3 Profiles of the measured and predicted temperature

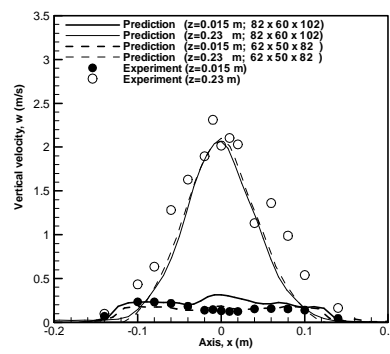


Figure 4 Profiles of the measured and predicted longitudinal velocity

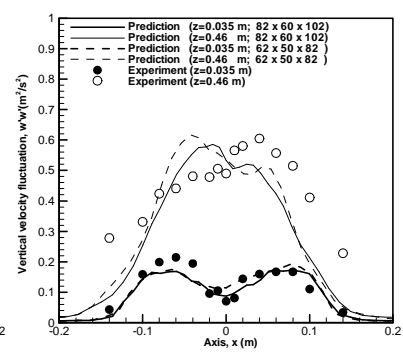


Figure 5. Profiles of the measured and predicted longitudinal velocity fluctuation

In Figure 6, we have plotted CO predicted in a traverse versus radial position at $H=0.12$ m and at the centreline against the average mixture fraction, Z , for a propane pool fire of 178 kW [4]. The predicted profiles exhibit the same similarity that is observed experimentally [4]. The soot volume fraction versus radial position in a traverse at $H=0.12$ m above the propylene pool fire are shown in Figure 7. The predicted and measured propylene data [4] show a high degree of similarity, consistent with our hypothesis that the smoke point is the controlling parameter for soot formation.

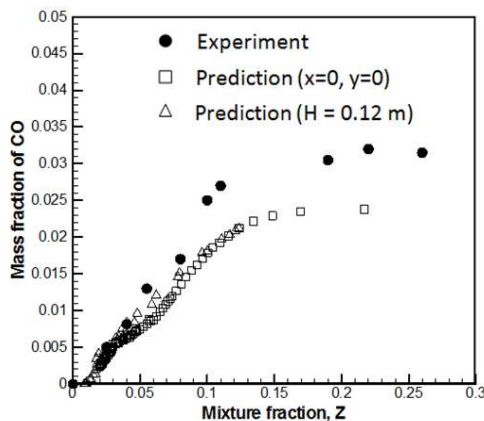


Figure 6. Comparison between the measured and predicted CO mass fraction as a function of the mixture fraction

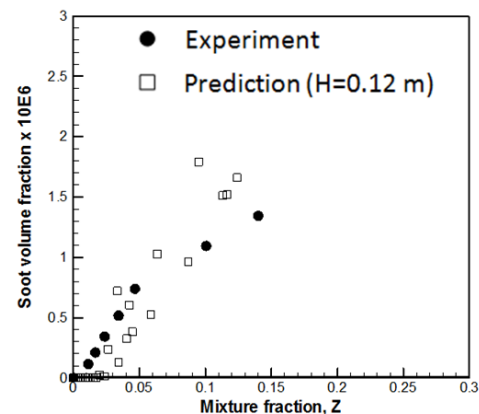


Figure 7. Comparison between the measured and predicted soot volume fraction as a function of the mixture fraction

For the pool-fire in crossflow [1], the flame shape, characterized by the flame height, H_f , and length, L_f , as defined in Figure 8, is compared to the experimental data from a gas burner fire with a length of $x_b=0.25$ m and a width of 0.4 m, giving a HRR of 45 kW. According to the experiment [1], the persistent flame regime corresponds to a gas temperature of about 450 - 500°C. By using this criterion, the predicted mean flame height/length are compared with the experimentally-determined ones in Figure 9 for the different wind velocities. Both the experiment and prediction show that the flame length progressively increases, and however, the flame height decreases with an increase of the wind velocity. The predicted and measured mean flame-surface heat flux downstream behind the burner ($x-x_b>0$), along the burning wall centerline ($y=0.2$ m) is presented in Figure 10. In spite of the discrepancy, the magnitude and distribution of the heat flux closely follow the general behaviour of the experimental data in a range of wind velocity from 0.7 to 2.5 m/s. The total heat flux, as a whole, is proportional to the wind velocity mainly due to an increase of the flame length.

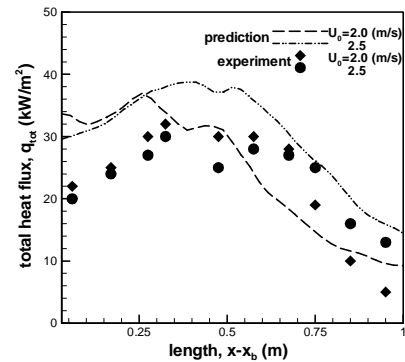
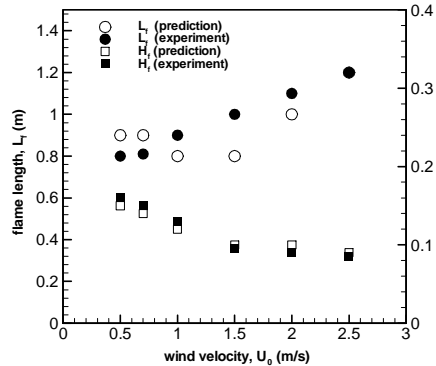
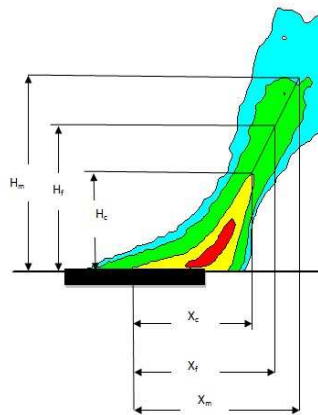
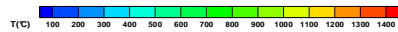


Figure 8. Flame shape of a pool-like fire in crossflow

Figure 9. Comparison between the predicted and measured flame height/length

Figure 10. Comparison between predicted and measured total heat flux

The instantaneous shape of the flame from the liquid fuel in the plane perpendicular to the fuselage for two wind speeds ($U_0=2$ and 10 m/s) is illustrated in Figure 11. For a low Froude number flame ($U_0=2$ m/s), surrounding the cone of fuel vapour is a zone of luminous persistent flame. Above this zone is a further combustion region, but here there is intermittency and obvious turbulence in the flaming. Finally there is the non-reacting buoyant plume, which is generally turbulent in nature and characterized by decreasing velocity and temperature with height. Wake regions are formed downstream of the plume and at times, spiralling vortex flows are seen in the plume. In the natural convection limit, as the Froude number increases, coherent structures appear also surrounding the cone of fuel vapour, the flame presenting a pronounced instability due to crossflow. Globally, the approach of LES is capable of reproducing the mechanism generating the buoyant instability present in the early development of the flame and the transition to turbulence far away from the fire source.

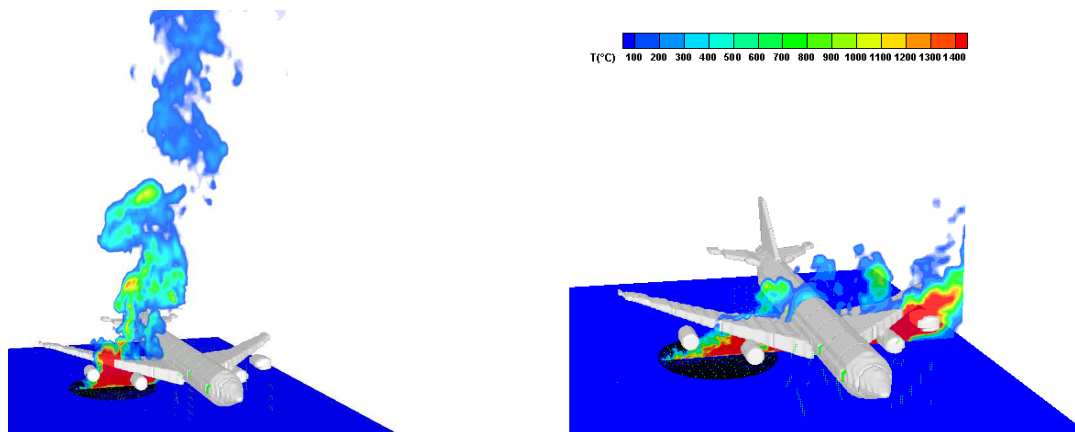


Figure 11. Instantaneous view of the predicted temperature with wind speed of 2 and 10 m/s

The calculated mean temperature contours on the plane perpendicular to the aircraft moving direction are presented in Figure 12(a-d). With the presence of a low wind speed ($U_0=2$ m/s), the quiescent pool fire consists of a buoyancy dominated flame zone with a peak temperature of 1200°C . The cross-flow is significantly deflected near the fire source as a result of an enhanced thermal blockage by the buoyancy forces. For the medium wind speed ($U_0=5$ m/s), the flame is elongated in the downstream

direction, and the region directly surrounding just in front of the aircraft is immersed in the highest temperature zone with a peak temperature of 1400°C due to complex wind/vorticity interactions. This situation induces an increase of the flame cover on the upper leeward side of the fuselage, resulting in the higher temperatures (700°C) there. The high wind speed ($U_0=10\text{ m/s}$) enhances the interaction between the cross-flow and the aircraft, and consequently, creates complex turbulent flow conditions. This situation facilitates the global flame shape alterations, which are combined with global enhancements in turbulent mixing. The windward flow is strongly accelerated over the top of the fuselage, and a low temperature region (300°C) occurs there due to increased convective transport. Besides, the fuel-rich flow is ejected from underneath of the aircraft, and this creates a second high temperature zone (1400°C) on the leeward side of the fuselage due to enhanced mixing by the presence of the vortices in the wake behind the aircraft, causing the flame zone to impinge on the bottom surface of the fuselage.

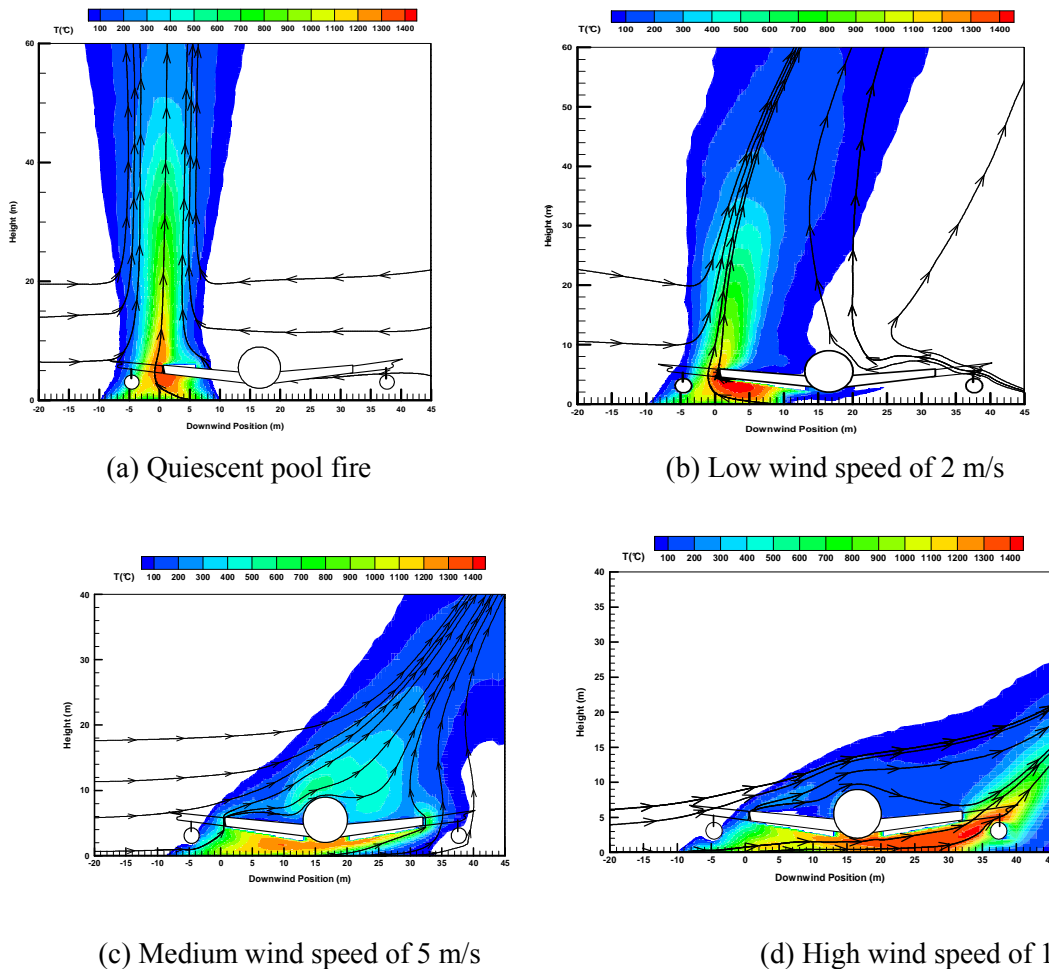


Figure 12. Contours of the time averaged temperature for different wind speed

Evolution of the heat release rate (HRR) generated from the pool fire and the peak in heat flux over the fuselage skin as a function of the pool diameter for different wind speeds is shown in Figures 13 and 14. As the pool size is below 20 m in diameter, the HRR is practically independent of the wind speed because the buoyancy-induced air entrainment is sufficient for providing an efficient mixing of fuel to air. The peak in heat flux over the fuselage skin becomes significant only when the pool size exceeds 30 m in diameter. The wind can alter the plume's dilution as well as plume-ambient momentum exchange and entrainment phenomena once the pool size surpasses a critical value of 20 m. The peak in heat flux over the fuselage skin becomes strong starting from the pool size of 20 m.

For the pool size of 40 m in diameter, the wind-assisted fire exhibits the highest HRR of about 4000 MW, and the quiescent pool fire gives the lowest of about 3500 MW due to the decaying of combustion efficiency which controls the heat generation during the fire. For the wind speed beyond 5 m/s, an increase of the peak in heat flux from 200 to 340 kW/m² is brought about with an increase of the pool size from 10 to 20 m due to increase in the HRR. Globally, an increase of the pool size enhances significantly the heat flux over the fuselage skin and HRR in a variety of the wind conditions.

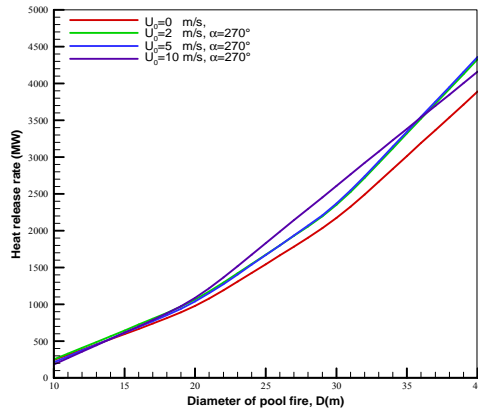


Figure 13. Evolution of the predicted heat release rate as a function of the pool fire size

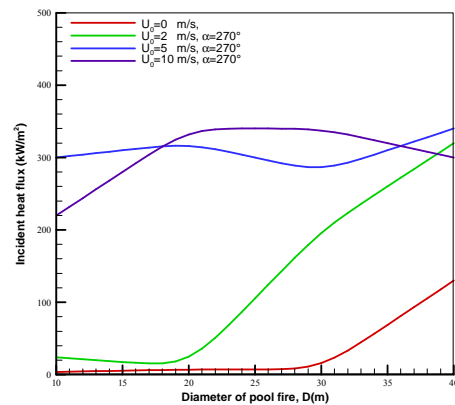


Figure 14. Evolution of the predicted incident heat flux as a function of the pool fire size

5. Conclusion

The model conforms to the large body of data in the literature showing that the fuel smoke point correlates the release of soot and concentration of CO is correlated well with mixture fraction. The free-stream turbulence in the boundary layer, which is erratic in nature, should be further investigated because it contribute to the large spatial and temporal variations of the flame shape and heat flux in a real aircraft fire situation.

References

- [1] G. Kolb, J.L. Torero, J.M. Most and P. Joulain (1997). Cross flow effects on the flame height of an intermediate scale diffusion flame, Proceedings of the International Symposium on Fire and Technology, Seoul, Korea, pp.169-177.
- [2] J.M. Suo-Anttila, L. Gritzo (2011). The effects of wind on fire environments containing large cylinders. Combustion Science and Technology, 181:1, 68-77.
- [3] M.O. Annarumma, J.M. Most and P. Joulain (1991). On the numerical modeling of buoyancy-dominated turbulent vertical diffusion flames. Combustion and Flame, 85, p. 403.
- [4] L. Orloff, J. de Ris and M.A. Delichatsios (1987). Chemical effects on molecular species concentrations in turbulent fires. Combustion and Flame, 69:273-289.
- [5] K. McGrattan (2014). Fire Dynamics Simulator – Technical Reference Guide, NIST Special Publication 1018.
- [6] T. Beji, J. Zhang and M.A. Delichatsios (2008). Determination of soot formation rate from laminar smoke point measurements. Comb Sci and Tech, 180(5):927-940.